PROCEEDINGS OF SPIE

SPIEDigitalLibrary.org/conference-proceedings-of-spie

The Imaging X-Ray Polarimetry Explorer (IXPE): technical overview IV

Brian Ramsey, Primo Attina, Luca Baldini, Mattia Barbanera, Wayne Baumgartner, et al.

Brian D. Ramsey, Primo Attina, Luca Baldini, Mattia Barbanera, Wayne H. Baumgartner, Ronaldo Bellazzini, Jeff Bladt, Stephen D. Bongiorno, Alessandro Brez, Simone Castellano, Rita Carpentiero, Marco Castronuovo, Luca Cavalli, Elisabetta Cavazutti, Fabio D'Amico, Saverio Citraro, Enrico Costa, William D. Deininger, Elisa D'Alba, Ettore Delmonte, Kurtis L. Dietz, Niccolo Di Lalla, Alessandro Di Marco, Giusseppe Di Persio, Immacolata Donnarumma, Sergio Fabiani, Riccardo Ferrazzoli, Joseph Footdale, Michael Head, William Kalinowski, Jeffery J. Kolodziejczak, Luca Latronico, Carlo Lefevre, Paolo Lorenzi, Leonardo Lucchesi, Simone Maldera, Alberto Manfreda, Elio Mangravati, Herman L. Marshall, Giorgio Matt, Massimo Minuti, Rondal Mize, Fabio Muleri, Hikmat Nasimi, Barbara Negri, Alessio Nuti, Stephen O'Dell, Leonardo Orsini, Darren Osborne, Christina Pentz, Maura Pilia, Matteo Perri, Melissa Pesce-Rollins, Colin Peterson, Michele Pinchera, Simonetta Puccetti, John Rankin, Ajay Ratheesh, Roger W. Romani, Paolo Sarra, Francesco Santoli, Andrea Sciortino, Christopher Schroeder, Carmelo Sgro, Paolo Soffitta, Gloria Spandre, Allyn Tennant, Antonino Tobia, Nicholas E. Thomas, Alessio Trois, Marco Vimercati, Jeffery Wedmore, Martin C. Weisskopf, Fei Xie, Francesco Zanetti, Cheryl Alexander, D. Zachery Allen, Fabrizio Amici, Jason Andersen, Angelo Antonelli, Spencer Antoniak, Matteo Bachetti, Randy M. Baggett, Rafaella Bonino, Christopher Boree, Fabio Borotto, Shawn Breeding, Daniele Brienza, H. Kyle Byggott, Ciro Caporale, Claudia Cardelli, Marco Ceccanti, Mauro Centrone, David Dolan, Yuri Evangelista, Kevin Ferrant, MacKenzie Ferrie, Brent Forsyth, Michelle Foster, Benjamin Garelick, Shuichi Gunji, Eli Gurnee, Grant Hibbard, Samantha Johnson, Eric Kelly, Kiranmayee Kilaru, Fabio La Monaca, Shelley Le Roy, Pasqualino Lofredo, Tyler Maddox, Guido Magazzu, Marco Marengo, Alessandra Marrocchesi, Francesco Massaro, David Mauger, Jeffrey McCracken, Michael McEachen, Paolo Mereu, Scott Mitchell, Ikuyuki Mitsuishi, Alfredo Morbidini, Federico Mosti, Toan Nguyen, Michela Negro, Isaac Nitschke, Mitch Onizuka, Chiara Oppedisano, Richard Pacheco, Alessandro Paggi, Will Painter, Steven D. Pavelitz, Raffaele Piazzolla, Alessandro Profeti, Jaganathan Ranganathan, Lee Reedy, Noah Root, Alda Rubini, Stephanie Ruswick, Javier Sanchez, Emanuele Scalise, Tim Seek, Kalie Sosdian, Chet O. Speegle, Toru Tamagawa, Marcello Tardiola, Robert Valerie, Amy L. Walden, Bruce Weddendorf, David Welch, "The Imaging X-Ray Polarimetry Explorer (IXPE): technical overview IV," Proc. SPIE 11821, UV, X-Ray, and Gamma-Ray Space Instrumentation for Astronomy XXII, 118210M (24 August 2021); doi: 10.1117/12.2595302

SPIE.

Event: SPIE Optical Engineering + Applications, 2021, San Diego, California, United States

The Imaging X-Ray Polarimetry Explorer (IXPE): Technical Overview IV

Brian D. Ramsey [1a], Primo Attina' [2], Luca Baldini [4,3], Mattia Barbanera [3], Wayne H. Baumgartner [1], Ronaldo Bellazzini [3], Jeff Bladt [5], Stephen D. Bongiorno [1], Alessandro Brez [3], Simone Castellano [3], Rita Carpentiero [6], Marco Castronuovo [6], Luca Cavalli [7], Elisabetta Cavazzuti [6], Fabio D' Amico [6], Saverio Citraro [3], Enrico Costa [8], William D. Deininger [5], Elisa D'Alba [7], Ettore Del Monte [8], Kurtis L. Dietz [1], Niccolo' Di Lalla [18], Alessandro Di Marco [8], Giuseppe Di Persio [8], Immacolata Donnarumma [6], Sergio Fabiani [8], Riccardo Ferrazzoli [8], Joseph Footdale [5], Michael Head [5], William Kalinowski [5], Jeffery J. Kolodziejczak [1], Luca Latronico [9], Carlo Lefevre [8], Paolo Lorenzi [7], Leonardo Lucchesi [3], Simone Maldera [9], Alberto Manfreda [3], Elio Mangraviti [7], Herman L. Marshall [10], Giorgio Matt [11], Massimo Minuti [3], Rondal Mize [1], Fabio Muleri [8], Hikmat Nasimi [3], Barbara Negri [6], Alessio Nuti [3], Stephen L. O'Dell [1], Leonardo Orsini [3], Darren Osborne [12], Christina Pentz [5], Maura Pilia [13], Matteo Perri [14], Melissa Pesce-Rollins [3], Colin Peterson [5], Michele Pinchera [3], Simonetta Puccetti [15], John Rankin [8,16], Ajay Ratheesh [8,17], Roger W. Romani [18], Paolo Sarra [7], Francesco Santoli [8], Andrea Sciortino [7], Christopher Schroeder [5], Carmelo Sgro' [3], Paolo Soffitta [8], Gloria Spandre [3], Allyn Tennant [1], Antonino Tobia [8], Nicholas E. Thomas [1], Alessio Trois [13], Marco Vimercati [7], Jeffrey Wedmore [5],Martin C. Weisskopf [1], Fei Xie [8], Francesco Zanetti [7], Cheryl Alexander [19], D. Zachery Allen [5], Fabrizio Amici [8], Jason Andersen [5], Angelo Antonelli [14], Spencer Antoniak [5], Matteo Bachetti [13], Randy M. Baggett [1], Raffaella Bonino [9,20], Christopher Boree [5], Fabio Borotto [9], Shawn Breeding [1], Daniele Brienza [8], H. Kyle Bygott [5], Ciro Caporale [9], Claudia Cardelli [3], Marco Ceccanti [3], Mauro Centrone [14], David Dolan [5], Yuri Evangelista [8], Kevin Ferrant [5], MacKenzie Ferrie [5], Brent Forsyth [12], Michelle Foster [1], Benjamin Garelick [5], Shuichi Gunji [21], Eli Gurnee [5], Grant Hibbard [5], Samantha Johnson [1], Erik Kelly [5], Kiranmayee Kilaru [22], Fabio La Monaca [8], Shelley Le Roy [23], Pasqualino Loffredo [8], Tyler Maddox [5], Guido Magazzu [3], Marco Marengo [9], Alessandra Marrocchesi [3], Francesco Massaro [9,20], David Mauger [5], Jeffrey McCracken [19], Michael McEachen [24], Paolo Mereu [9], Scott Mitchell [5], Ikuyuki Mitsuishi [25], Alfredo Morbidini [8], Federico Mosti [9], Toan Nguyen [5], Michela Negro [9,20], Isaac Nitschke [5], Mitch Onizuka [5], Chiara Oppedisano [9], Richard Pacheco [5], Alessandro Paggi [9,20], Will Painter [5], Steven D. Pavelitz [1], Raffaele Piazzolla [6], Alessandro Profeti [3], Jaganathan Ranganathan [1], Lee Reedy [12], Noah Root [5], Alda Rubini [8], Stephanie Ruswick [12], Javier Sanchez [23], Emanuele Scalise [8], Tim Seek [5], Kalie Sosdian [5], Chet O. Speegle [1], Toru Tamagawa [26], Marcello Tardiola [9], Robert Valerie [5], Amy L. Walden [1], Bruce Weddendorf [27], David Welch [12]

[1] NASA Marshall Space Flight Ctr., Huntsville, AL 35812, USA
[2] INAF Osservatorio Astrofisico di Torino, Strada Osservatorio 20, 10025 Pino Torinese (TO), Italy
[3] Istituto Nazionale di Fisica Nucleare - Pisa, Largo Bruno Pontecorvo 3, 56127 Pisa (PI), Italy
[4] Universita' di Pisa, Lungarno Antonio Pacinotti 43, 56126 Pisa (PI), Italy
[5] Ball Aerospace, 1600 Commerce Street, Boulder, CO 80301 USA
[6] Agenzia Spaziale Italiana, Via del Politecnico, 00133 Roma (RM), Italy
[7] OHB Italia SpA, Via Gallarate 150, 20151 Milano (MI), Italy

[a] Contact Author: Brian.Ramsey@nasa.gov, Tel: (256)-961-7784. Address: 320 Sparkman Drive, Huntsville, Al 35805.

UV, X-Ray, and Gamma-Ray Space Instrumentation for Astronomy XXII, edited by Oswald H. Siegmund, Proc. of SPIE Vol. 11821, 118210M · © 2021 SPIE
CCC code: 0277-786X/21/$21 · doi: 10.1117/12.2595302

[8] INAF Istituto di Astrofisica e Planetologia Spaziali, Via del Fosso del Cavaliere 100, 00133 Roma (RM), Italy
[9] Istituto Nazionale di Fisica Nucleare - Torino, Via Pietro Giuria 1, 10125 Torino (TO), Italy
[10] Massachusetts Institute of Technology, 77 Massachusetts Avenue, Cambridge, MA 02139, USA
[11] Universita' degli Studi Roma Tre, Via della Vasca Navale 84, 00146 Roma (RM), Italy l Lab. for Atmospheric and Space Physics, 1234 Innovation Drive, Boulder, CO 80303, USA
[12] Lab. for Atmospheric and Space Physics, 1234 Innovation Drive, Boulder, CO 80303, USA
[13] INAF Osservatorio Astronomico di Cagliari, Via della Scienza 5, 09047 Selargius (CA), Italy
[14] INAF Osservatorio Astronomico di Roma, Via Frascati 33, 00078 Monte Porzio Catone (RM), Italy
[15] ASI Space Science Data Ctr., Via del Politecnico, Edificio D, 00133 Roma (RM), Italy
[16] Universita' di Roma "La Sapienza", Piazzale Aldo Moro 5, 00185 Roma (RM) Italy
[17] Universita' degli Studi di Roma "Tor Vergata", Via Lucullo, 11, 00187 Roma (RM), Italy
[18] Stanford University, 382 Via Pueblo Mall, Stanford, CA 94305-4060, USA
[19] Linc Research, Marshall Space Flight Ctr., Huntsville, AL 35812, USA
[20] Universita' degli Studi di Torino, Via Giuseppe Verdi 8, 10124 Torino (TO), Italy
[21] Yamagata University, 1-4-12 Kojirakawa-machi, Yamagata-shi, 990-8560, Japan
[22] USRA, Marshall Space Flight Ctr., Huntsville, AL 35812, USA
[23] ESSCA, Marshall Space Flight Ctr., Huntsville, AL 35812, USA
[24] Northrop Grumman Innovation Systems, 600 Pine Avenue, Goleta, CA 93117, USA
[25] Nagoya University, Furo-cho, Chikusa-ku, Nagoya, 464-8602, Japan
[26] RIKEN Nishina Ctr., 2-1 Hirosawa, Wako, Saitama 351-0198, Japan
[27] Weddendorf Design, 14060 Valley Vista Drive, Huntsville, AL 35803, USA

ABSTRACT

Scheduled to launch in late 2021, the Imaging X-ray Polarimetry Explorer (IXPE) is a Small Explorer Mission designed to open up a new window of investigation -- X-ray polarimetry. The IXPE observatory features 3 identical telescopes each consisting of a mirror module assembly with a polarization-sensitive imaging x-ray detector at its focus. An extending boom, deployed on orbit, provides the necessary 4 m focal length. The payload sits atop a 3-axis stabilized spacecraft which, among other things, provides power, attitude determination and control, commanding, and telemetry to the ground. During its 2-year baseline mission, IXPE will conduct precise polarimetry for samples of multiple categories of x-ray sources, with follow-on observations of selected targets. IXPE is a partnership between NASA and the Italian Space Agency (ASI).

Keywords: X-ray polarimetry, gas pixel detectors, grazing-incidence optics

1. INTRODUCTION

The Imaging X-Ray Polarimetry Explorer[1] (IXPE) is a NASA small explorer mission selected in early 2017. IXPE will be a pathfinder mission opening a new window on the x-ray sky by enabling polarimetry measurements on essentially all classes of the brightest cosmic x-ray sources. Scheduled for launch in late 2021, with a 2-year baseline mission, IXPE will perform a study of approximately 50 sources in its first year, with follow-on more detailed observations of selected targets in year two.

The following technical overview provides brief programmatic details (section 2), a detailed description of the payload and its calibration (section 3), an overview of the Ball-Aerospace-provided spacecraft (section 4), and a discussion of the

ground network for observatory commanding, data retrieval, and processing (section 5). Finally, the overview concludes with the current status of the program as of July 2021.

2. PROGRAM OVERVIEW

The IXPE observatory will be launched on a Falcon-9 rocket from Kennedy Space Center in late 2021. It will be inserted into an equatorial orbit at a nominal altitude of 600 km and a nominal inclination of 0°. This orbit inclination provides a low charged-particle background and allows frequent data downloads to the primary ground station in Malindi, Kenya (a backup ground station is in Singapore). The chosen altitude maximizes the orbit lifetime while still satisfying a NASA requirement of re-entry within 25 years.

The IXPE Mission Operations Center will be at the University of Colorado Laboratory for Atmospheric and Space Physics (LASP) while the Science Operations Center will be at the Marshall Space Flight Center (MSFC). Data will be archived at NASA's High Energy Astrophysics Science Archive Center (HEASARC) and made publicly available within 30 days of the end of an observation for the first 3 months, and within 1 week of an observation after that.

NASA's Small Explorers are P.I.-led missions, with the P.I team, program management, system engineering, and safety and mission assurance oversight all at MSFC. In addition, MSFC is responsible for the Mirror Module Assembly (MMA) fabrication, testing, and calibration, as well as for science operations and data analysis. Archiving will be the responsibility of NASA's HEASARC. The program also has a substantial contribution from the Italian Space Agency, which provides funding for the polarization-sensitive detectors as well as the Malindi ground station and scientific support with its Space Science Data Center (SSDC). The IXPE spacecraft is provided by Ball Aerospace, which is also responsible for observatory integration and testing. Finally, to aid in science planning, IXPE has a large science advisory team, comprising of more than 90 scientists from 12 countries.

3. THE IXPE PAYLOAD

3.1 Overview

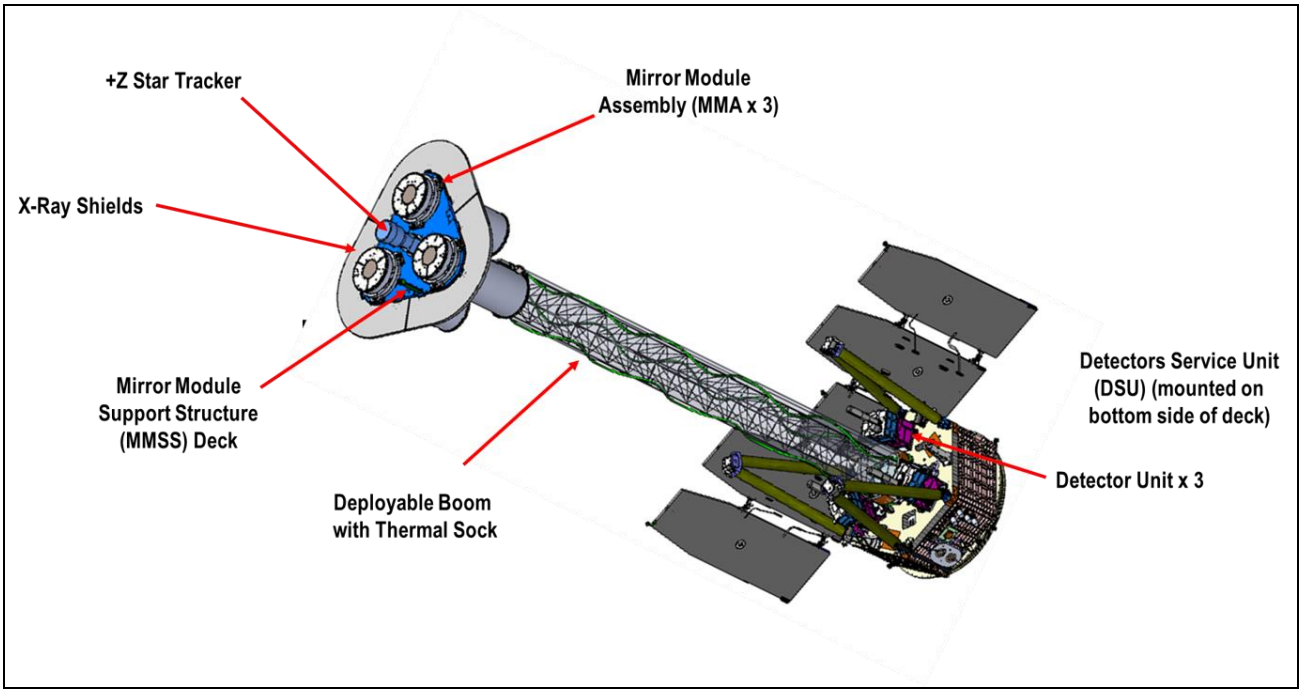

Figure 1: The IXPE Observatory highlighting the payload elements

Figure 1 shows a schematic of the IXPE observatory. The payload consists of three identical x-ray telescopes each comprised of a Mirror Module Assembly (MMA) with a polarization-sensitive detector unit (DU) at its focus. Data from

the three detectors are handled by a Detectors Service Unit (DSU), located under the spacecraft top deck, which packages the data for the S/C computer provides for transmission to the ground. A deployable boom establishes the appropriate focal length after launch- and positions each MMA above its respective detector. Fixed X-ray shields, in combination with collimators on each detector, limit stray radiation so that only x-ray photons that enter through the mirror can impinge on the detector entrance window. A star tracker on each end (rear star tracker which points in the -Z direction not shown in Figure 1) provide pointing knowledge for the three-axis stabilized spacecraft.

3.2 Mirror Module Assembly

The IXPE observatory has three MMAs[2,3] each comprised of 24 concentrically-nested mirror shells. The mirror shells are fabricated from an electroforming process using a nickel/cobalt alloy that has a higher strength than more-typically-used pure nickel. The shells are closely packed, with just 2 mm separation, to maximize the effective area for a given outer diameter. Each mirror shell has an overall length of 600 mm which includes both parabolic and hyperbolic segments of the Wolter-1 configuration. Table 1 gives the MMA parameters with performance data - effective area and angular resolution - from MMA calibrations.

Table 1: Mirror Module Assembly parameters

Parameter	Value
Number of mirror modules	3
Number of shells per mirror module	24
Focal length	4 m
Total shell length	600 mm
Range of shell diameters	162–272 mm
Range of shell thicknesses	0.18–0.25 mm
Shell material	Electroformed nickel–cobalt alloy
Effective area per mirror module	166 cm^2 (@ 2.3 keV); > 175 cm^2 (3–6 keV)
Angular resolution (HPD)	≤ 28 arcsec
Field of view (detector limited)	12.9 arcmin square

The mechanical design of each MMA is shown in Figure 2. The front spider is the primary structural element of the design, through which the MMA will mount to the mirror module support structure during payload integration at spacecraft supplier and integrator, Ball Aerospace. Each of the nine spokes of the front spider has a precisely fabricated and positioned comb glued to it. During MMA alignment and assembly, each mirror shell is inserted and glued into the corresponding slot between the tines of each comb, thus mounting the mirror shells to the spokes of the front spider.

The rear spider has 18 spokes, each with a metal comb. After all of the 24 shells have been epoxied to the front spider, the rear spider is attached to the central support tube and its metal combs aligned such that each mirror shell floats within the corresponding slot between the tines of the rear-spider combs. However, unlike the front-spider combs, which hold the mirror shells, the rear-spider combs merely limit excursions of the shells under launch loads to preclude shell-to-shell collisions. In this way the mirror shells are not over-constrained, as they would be if rigidly attached at both ends. To prevent any possible marring of the mirror shell surface the comb tines have heat-shrink sleeving applied to cushion impacts.

Completing the MMA is a pair of thermal shields, one at each end. These are fabricated from an ultra-thin (1.4 µm) polyimide film, coated with 50 nm of aluminum and supported on a highly transparent steel mesh. A contribution from Nagoya University in Japan, they provide for thermal control, restricting heat loss while allowing x-rays to pass though[4].

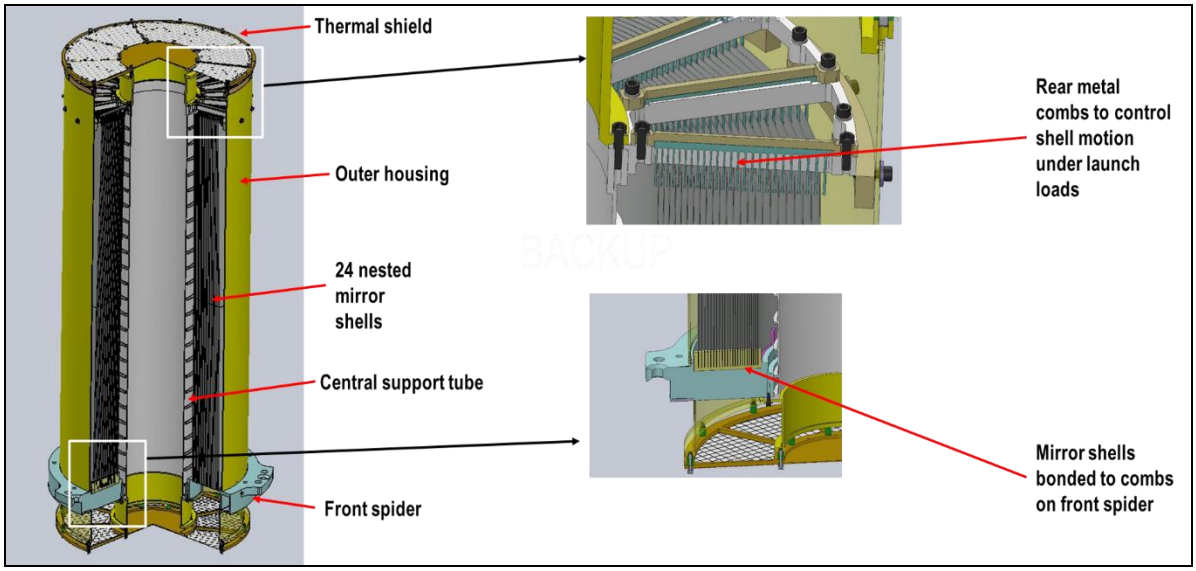

Figure 2: Mechanical design of the MMA

3.3 Detector Units

The heart of the IXPE payload are the detector units (DUs). Located at the focus of each MMA these provide position sensitivity, energy determination, timing information and, most importantly, polarization sensitivity. Inside each DU is a Gas Pixel Detector[5,6,7] (GPD) which images the photoelectron tracks produced by x-rays absorbed in the special fill gas (Dimethyl Ether - DME). The initial emission direction of the photoelectron contains the necessary information to determine the polarization of the source, while the initial interaction point and the total charge in the track provide the location and energy of the absorbed x ray, respectively.

Figure 3 shows a schematic of the GPD. An x ray enters through a beryllium window and interacts in the DME fill gas. The resulting photoelectron leaves a trail of ionization, and this photoelectron track drifts through a Gas Electron Multiplier (GEM), to provide charge gain, and onto a pixel anode readout. Table 2 gives the relevant performance parameters.

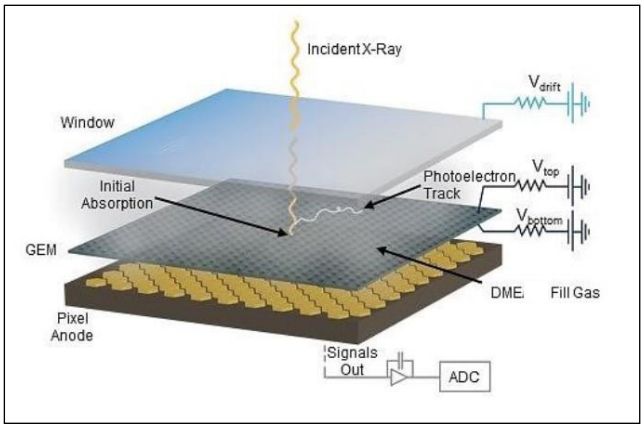

Figure 3: Schematic of the Gas Pixel Detector (GPD)

Table 2: Performance parameters of an IXPE Detector Unit (DU)

Parameter	Value
Sensitive area	15 mm × 15 mm (13 x 13 arcmin)
Fill gas and asymptotic pressure	DME @ 0.656 atmosphere
Detector window	50-μm thick beryllium
Absorption and drift region depth	10 mm
Spatial resolution (FWHM)	≤ 123 μm (6.4 arcsec) @ 2 keV
Energy resolution (FWHM)	0.57 keV @ 2 keV ($\propto \sqrt{E}$)
Useful energy range	2 - 8 keV

An expanded view of a detector unit is shown in Figure 4 (left). As well as the GPD, the unit houses all of the back-end electronics to process each event, as well as high-voltage power supplies. It also houses a filter and calibration wheel assembly for on-orbit calibration (see section 3.7), as well as a collimator for reduction of x-ray background. Figure 4 (right) shows a photograph of a completed flight DU.

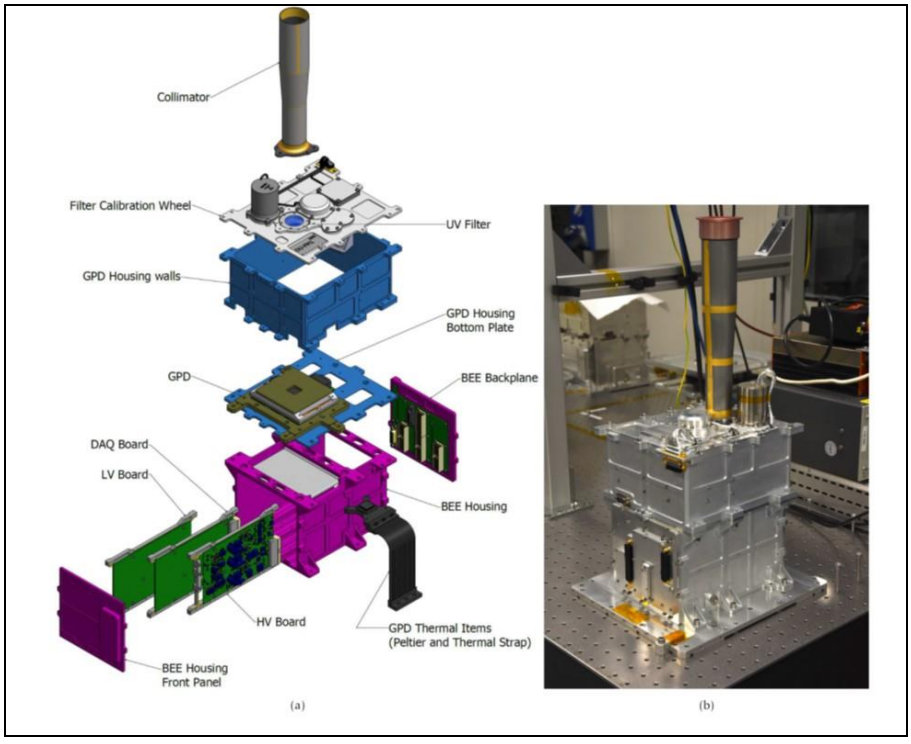

Figure 4: Expanded view of a Detector Unit (DU, left); photograph of a completed flight unit (right).

3.4 Extending Boom

To fit within the original launch vehicle fairing and yet provide the necessary 4-m focal length, IXPE utilizes an extending boom that deploys on orbit. The boom, provided by Northrop Grumman Space Systems, is triangular in section, with three glass-fiber longerons that extend along its full length. Battens and diagonals complete the structure and provide additional stiffness.

The boom is initially coiled in a canister and when released uncoils via stored strain energy in a controlled manner via a lanyard and a damper which governs the deployment speed. The lanyard is also used to stow the boom after ground tests. Covering the boom is a thermal sock which limits sun/shade temperature excursions and thereby limits diurnal changes in overall length. Atop the boom is a tip/tilt/rotate mechanism that may be used on orbit to adjust the initial alignment of the MMAs with respect to the DUs (see section 3.5).

3.5 Payload Alignment

The IXPE focal plane detector has an active area of 15 mm ×15 mm and so each telescope must be carefully aligned to ensure the image is near the center of the detector and that the axis of each mirror module is co-aligned with the star tracker. The driving requirement here is the capability to simultaneously place an extended source of diameter up to 9 arcminutes on all three detectors.

Alignment primarily consists of placing the three DUs and the three MMAs on congruent triangles, the former on the top deck of the spacecraft and the latter on the deployable mirror module support structure. Surface mount reflectors (SMRs) installed on the MMAs and DUs during construction enable this process which is done using a laser tracker system. Precise knowledge linking the SMR positions to the respective nodes of the MMAs and the DUs is derived to high precision (< 100 μm) during component assembly. Before the MMAs are placed precisely in position, their x-ray axes are co-aligned with each other and with the optical axis of the forward star tracker using alignment cubes mounted on each MMA and measured during x-ray calibration.

The deployment accuracy of the boom is such that the x-ray image of an on-axis x-ray source should be within ~ 1 mm (1-σ) of the center of each detector. For precise alignment, use may be made of an on-board Tip/Tilt/Rotate (TTR) system (Figure 5, left). Situated between the boom and the mirror module support structure, the TTR can effectively repoint the observatory to move the image on the detector as shown in Figure 5 (right). This is possible because the star tracker is mounted on the MMSS, so that adjusting the TTR in tip/tilt has the effect of offset point the observatory which then moves to re-acquire the target. The rotate component of the TTR compensates for any rotational offset when the boom deploys.

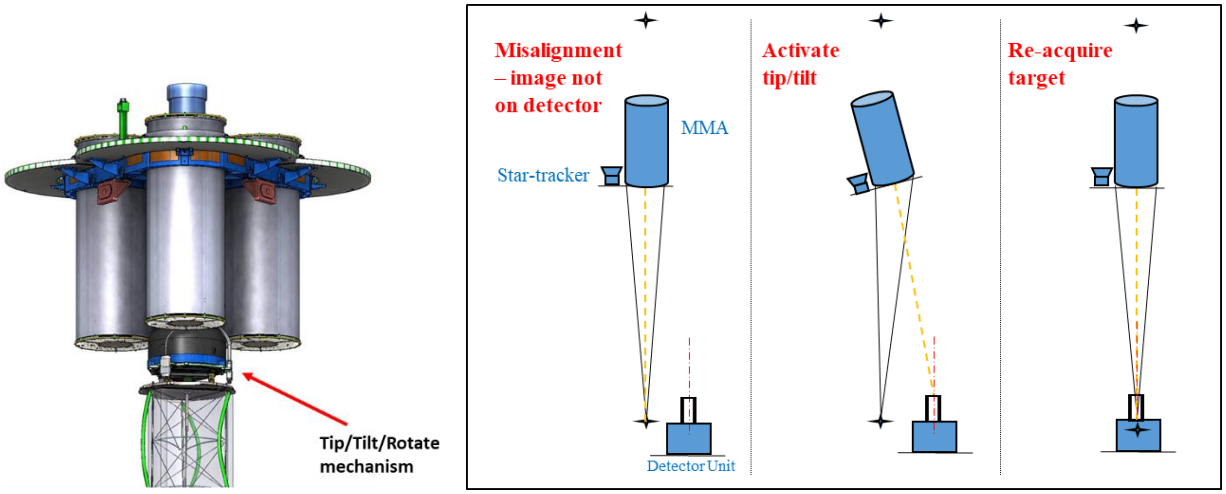

Figure 5: Left image shows the Tip/Tilt/Rotate mechanism; Right image shows the MMA on-orbit alignment scheme

3.6 Ground Calibration

Precise calibration of the x-ray telescopes is very important for subsequent on-orbit data analysis. This is particularly true for a pathfinder mission like IXPE where polarization will be measured for the first time from many sources. IXPE calibrations consisted of detailed detector calibrations in Italy and detailed MMA calibrations in the US. In addition, a single telescope consisting of the spare MMA and the Spare Detector Unit, was also calibrated in the US to confirm that its response could be synthesized from the individual MMA and DU calibration.

Detector Unit calibrations were carried out in Italy using purpose-built calibration equipment[8]. A key task for this was the development of a suite of polarized sources with precisely known polarization, that would cover the full IXPE energy range. These sources utilized matched x-ray energies with available crystals to give Bragg reflection at near 45°, resulting in near 100% polarized x rays. Details of these custom sources is given in Table 3.

DU flight-unit calibrations extended from July 2019 to March 2020. The spare unit completed calibration in September 2020. Measurements of the DU polarization response constituted approximately 77.5% of the total calibration time. Included in this was a large block of time (60% of the total) to map the DU polarization response to unpolarized x rays, so that any small systematic effects could be removed in flight data analysis.

Table 3: Custom polarized sources (crystal + x-ray tube) used in DU ground calibrations

Crystal	X-ray Tube	Energy (keV)	Diffraction Angle	Polarization (%)
PET (002)	Continuum	2.01	45.0	~ 100
InSb (111)	Mo L	2.29	46.4	99.2
Ge (111)	Rh L	2.70	44.9	~ 100
Si (111)	Ag L	2.98	41.6	95.1
Al (111)	Ca K	3.69	45.9	99.4
Si (220)	Ti K	4.51	45.7	99.5
Si (400)	Fe K	6.40	45.5	~ 100

MMA calibrations were carried out at the MSFC Stray Light Test Facility (SLTF), which features a 100-m vacuum beam tube with x-ray source assemblies at one end and a 10 m × 3 m test chamber at the other (see Figure 6). The MMA under calibration was mounted in the test chamber atop a hexapod that enabled precise linear control in all axes and precise angular control in tip and pan. Beyond the MMA, at a distance of 4.17 m (the effective focal length of the MMA at 100-m source distance), were the facility detectors used to measure the MMA response. These consisted of a fast silicon drift detector with known effective area and a CCD camera with fine (13.5 μm) pixels for accurate MMA point spread function measurements, both mounted on a moveable stage. After initial MMA calibrations the flight spare detector unit was also mounted on the detector stage.

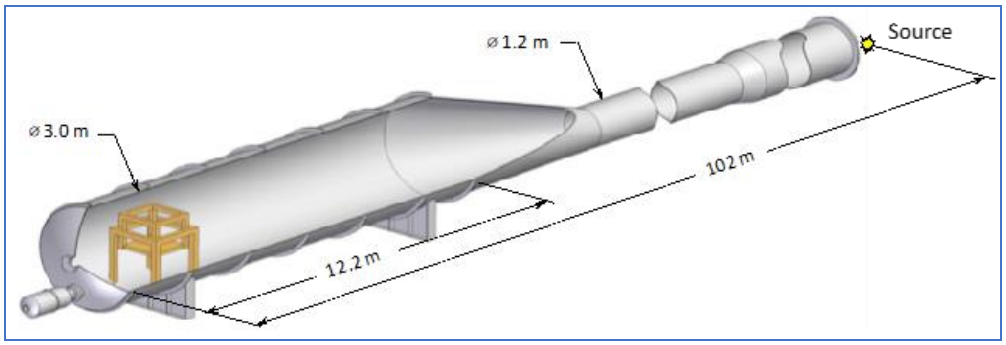

Figure 6: The MSFC Stray-Light Test Facility (SLTF)

Calibration measurements were made at multiple energies for on- and off-axis effective area and angular resolution. Also measured were the MMA responses to sources outside of the direct field of view, so called ghost rays, which can increase the observation background for observations in crowded source regions. For telescope calibration, a subset of the polarized source energies used in Italy (Rh, Ti and Fe) were utilized to measure the polarization response in addition to effective area and angular resolution. MSFC calibrations ran from July 2020 through January 2021. An important finding from the telescope calibration was, as expected, that the polarization response of the DU was not affected by the presence of the MMA.

3.7 In-Flight Calibration Monitoring

To enable in-flight calibration monitoring, each DU is equipped with a filter and calibration wheel assembly[9] (Figure 7). These assemblies contain various radioactive sources that can be rotated in front of the GPD to provide for monitoring gain, energy resolution, spurious modulation and modulation factor (the sensitivity to polarization for a 100% polarized source) during the mission. The calibration sources will be used in those parts of the orbit when the x-ray source under study is eclipsed by the earth, calibrating one detector per orbit.

The calibration sources are all based on ^{55}Fe isotopes which have a K_α line at 5.9 keV and a K_β line at 6.5 keV. Cal source A produces polarized x rays at 3 keV (via a silver target, Si Lα = 3 keV) and at 5.9 keV, through 45° Bragg reflection off a graphite mosaic crystal. Cal sources C and D are unpolarized 5.9 keV and 6.5 keV x rays in a spot (~ 3mm) and flood (~ 15 x 15 mm) configuration respectively. Cal source D utilizes a silicon target in front of the ^{55}Fe to produce a broad beam at 1.7 keV (Si K_α).

In addition to the calibration sources the wheel also contains an open position, a closed position and an attenuator position consisting of a 75-µm-thick kapton foil coated with 100 nm of aluminum on each side. The first of these is for normal operations, the second for internal background measurements and the third is for observing very bright sources which would otherwise exceed the throughput of the system

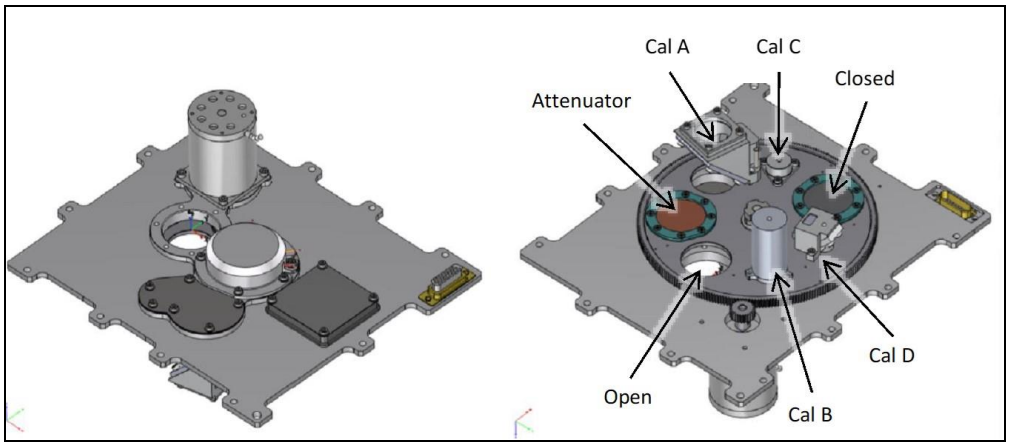

Figure 7: Filter and calibration wheel assembly (left: top view (+z); right: bottom view (-z))

4. THE IXPE SPACECRAFT

The IXPE spacecraft bus is Ball Aerospace's fourth build of its BCP-small spacecraft[10]. This design utilizes a hexagonal structure made from machined aluminum plates and closed out with a honeycomb top deck. Components are mounted inside the side panels as well as both sides of the top deck (see Figure 8). The solar array, shown unfurled, wraps around the spacecraft body for launch and prior to deployment.

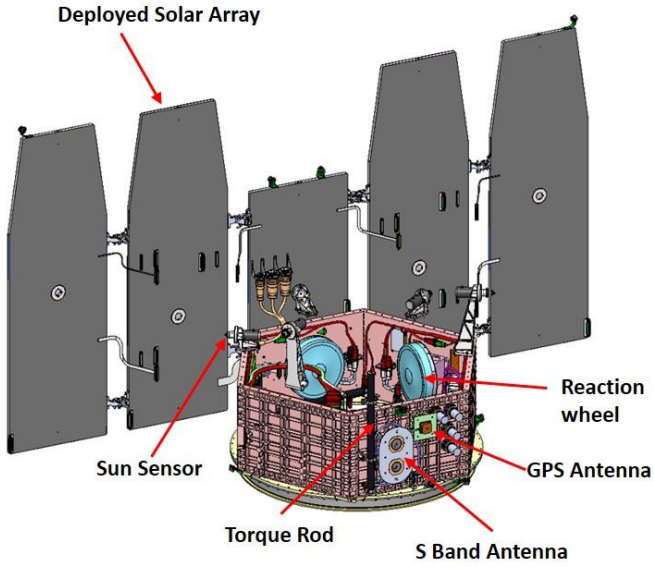

Figure 8: IXPE spacecraft schematic (shown with solar panels unfurled)

For coarse attitude sensing the IXPE spacecraft utilizes an array of 12 sun sensors and a 3-axis magnetometer. For fine attitude there are two star trackers, one on the mirror module support structure and co-aligned with the axes of the MMAs (see Figure 1), and one underneath the spacecraft and pointing in the -Z direction. Pointing control is via 3 reaction wheels with torque rods used to de-saturate the wheels as necessary.

Command and data handling is handled by an integrated avionics unit. This contains the flight software and handles the telemetry, data storage and overall payload control. Communication is via S band, with a 2 kbps command rate and a 2 Mbps downlink telemetry rate. There is 6 Gbytes of on-board memory assigned for data storage between downloads.

5. GROUND NETWORK

Communication with IXPE is via a primary ground station in Malindi, Kenya, with a backup station in Singapore. Data download will vary with observing program but will average around 3-4 contacts per day. Commanding will be approximately once per week.

Mission operations will be run from the Mission Operation Center (MOC) run by the Laboratory for Atmospheric and Space Physics (LASP) located at the University of Colorado. The MOC communicates with the Science Operations Center (SOC) and with the observatory via the ground network shown in Figure 9.

The SOC, located at NASA/MSFC, is responsible for science operations. The SOC formulates the observing plan that is then sent to the MOC for detailed scheduling. The SOC receives all the observatory data which it then processes. Science data products are then distributed to the HEASARC for public access within 1 week after the end of an observation (after an initial 3-month checkout period during which the turnaround time is 30 days)

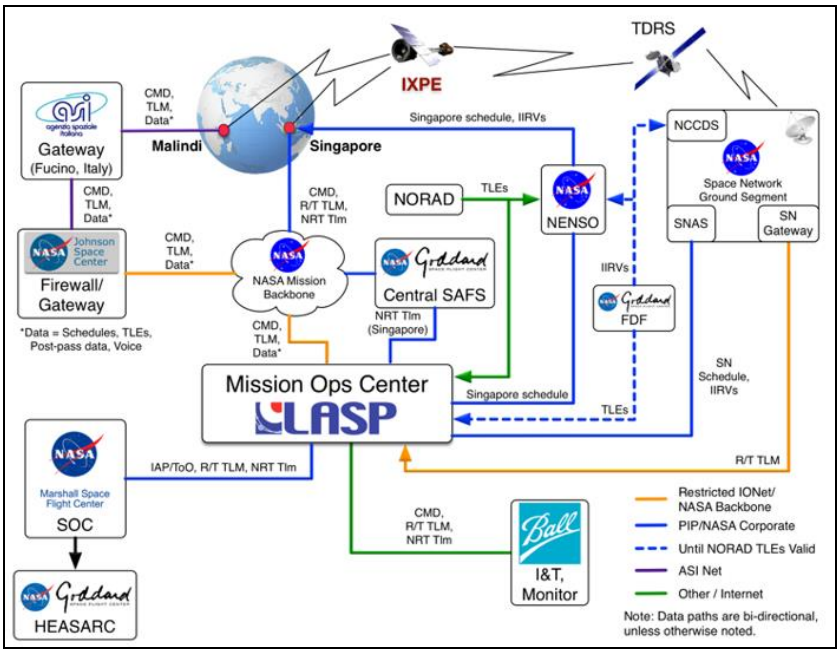

Figure 9: IXPE ground network

6. CURRENT STATUS

At the time of writing (July 2021), the IXPE observatory is fully integrated, has completed vibration, shock and acoustic testing and is about to enter a 22-day thermal vacuum test (see Figure 10). After all environmental testing is complete there will be a series of functional tests before shipment from Colorado to the Kennedy Space Center, which is currently scheduled for mid-October 2021 (contingent on the current launch date holding firm). Observatory test and integration at the SpaceX facility will take approximately 1 month.

Figure 10: IXPE observatory on vibration table (left) and being prepared thermal vacuum testing (right). Credit: Ball Aerospace.

7. REFERENCES

[1] Weisskopf, M. C., Ramsey, B., O'Dell, S., Tennant, A., Elsner, R., Soffitta, P., Bellazzini, R., Costa, E., Kolodziejczak, J., Kaspi, V., Muleri, F., Marshall, H., Matt, G., & Romani, R., "The Imaging X-ray Polarimetry Explorer (IXPE)," SPIE 9905, 17 10pp (2016).

[2] Ramsey, B.D., "Optics for the Imaging X-ray Polarimetry Explorer, SPIE 10399, 07, (2017)

[3] Ramsey, B.D., IXPE mirror module assemblies, SPIE 11119, 2, (2019)

[4] Mitsuishi, I., Futamura, T., Shimizu, S., Takehara, Y., Yamaguchi, T., Tawara, Y., Tamura, K., Onishi, T., Tachibana, K., Miyata, K., Tamagawa, T., Chiba, T., Tachibana, M., Murashima, K., & Tachikawa, S., "Development of the thermal shield for the optics on board the Imaging X-ray Polarimetry Explorer (IXPE)," SPIE 11119, paper 51 (2019).

[5] Costa, E., Soffitta, P., Bellazzini, R., Brez, A., Lumb, N., & Spandre, G., "An efficient photoelectric X-ray polarimeter for the study of black holes and neutron stars," Nature 411, 662-665 (2001).

[6] Bellazzini, R., Spandre, G., Minuti, M., Baldini, L., Brez, A., Latronico, L., Omodei, N., Razzano, M., Massai, M. M., Pesce-Rollins, M., Sgro, C., Costa, E., Soffitta, P., Sipila, H., & Lempinen, E., "A sealed Gas Pixel Detector for X-ray astronomy," NIMPA 579, 853-858 (2007).

[7] Baldini L., Barbanera M., Bellazzini R., Bonino R., Borotto F, Brez A., Caporale C., Cardelli C., Castellano S., Ceccanti M., Citraro S., Di Lalla N., Latronico L., Lucchesi L., Magazz`u C., Magazz`u G., Maldera S., Manfreda A., Marengo M., Marrocchesi A., Mereu P., Minuti M., Mosti F., Nasimi H., Nuti A., Oppedisano C., Orsini L., Pesce-Rollins M., Pinchera M., Profeti A., Sgr`o C., Spandre G., Tardiola M., Zanetti D., Amici F., Andersson H., Attin`a, P., Bachetti M., Baumgartner W., Brienza D., Carpentiero R., Castronuovo M., Cavalli L., Cavazzuti E., Centrone M., Costa E., D'Alba E., D'Amico F., Del Monte E., Di Cosimo S., Di Marco A., Di Persio G., Donnarumma I., Evangelista,Y., Fabiani S., Ferrazzoli R., Kitaguchi T., La Monaca F., Lefevre C., Loffredo P., Lorenzi P., Mangraviti E., Matt G., Meilahti T., Morbidini A., Muleri F., Nakano T., Negri B., Nenonen S., O'Dell S. L., Perri M., Piazzolla R., Pieraccini S., Pilia M., Puccetti S., Ramsey B. D., Rankin J., Ratheesh A., Rubini A., Santoli F., Sarra P., Scalise E., Sciortino A., Soffitta P., Tamagawa T., Tennant A., Tobia A., Trois A., Uchiyama K., Vimercati M., Weisskopf M. C., Xie F., Zanetti F., Zhou Y., arXiv, arXiv:2107.05496, to be published in Astroparticle Physics, (2021).

[8] Muleri, F., Lefevre, C., Piazzolla, R., Morbidini, A., Amici, F., Attina, P., Centrone, M., Del Monte, E., Di Cosimo, S., Di Persio, G., Evangelista, Y., Fabiani, S., Ferrazzoli, R., Loffredo, P., Maiolo, L., Maita, F., Primicino, L., Rankin, J., Rubini, A., Santoli, F., Soffitta, P., Tobia, A., Tortosa, A., & Trois, A., "Calibration of the IXPE instrument," SPIE 10699, 5C 11pp (2018).

[9] Ferrazzoli, R., Muleri, F., Lefevre, C., Morbidini, A., Amici, F., Brienza, D., Costa, E., Del Monte ,E., Di Marco, A., Di Persio, G., Donnarumma, I., Fabiani, S., La Monaca, F., Loffredo, P., Maiolo, L., Maita, F., Piazzolla, R., Ramsey, B., Rankin, J., Ratheesh, A., Rubini, A., Sarra, P., Soffitta, P., Tobia, A. & Xiea, F., "In-flight calibration system of imaging x-ray polarimetry explorer", J. Astron. Telesc. Instrum. Syst., Vol 6(4), (2020).

[10] Deininger, W., Kalinowski, W., Masciarelli, J., Gray, S., Peterson, C., Hibbard, G., Wedmore, J., Bladt, J., Weisskopf, M., Ramsey, B., O'Dell, S., Tennant, A., Mize, R., Foster, M., Soffitta, P., Muleri, F., Santoli, F., Del Monte, E., Baldini, L., Pinchera, M., Latronico, L., Trois, A. & Osborne, D., "IXPE Mission System Concept and Development Status ," Paper 2.0108-2104, 2020 IEEE Aerospace Conference, Big Sky, MT, USA, 7-14 March 2020.